Supporting Information for

Vapor Phase Hydrodeoxygenation of Furfural to 2-Methylfuran on Molybdenum Carbide Catalysts

Wen-Sheng Lee[1,3], Zhenshu Wang[1,3], Weiqing Zheng[2,3] , Dionisios G. Vlachos[2,3], Aditya Bhan[1,3,*]

[1]*Department of Chemical Engineering and Materials Science, University of Minnesota, Minneapolis, MN 55455, USA*

[2]*Department of Chemical and Biomolecular Engineering University of Delaware, Newark, DE, 19716, USA*

[3]*Catalysis Center for Energy Innovation*

*Corresponding Author: E-mail: abhan@umn.edu; Fax: (+1) 612-626-7246

1. Characterization of molybdenum carbide catalysts

Table S1. Independent CO chemisorption measurements for the Mo$_2$C samples listed in Table 1. These chemisorption data were also used to plot Figure 3(b).

Catalyst	aging time (days)	CO uptake at 423K or 323K (μmole g^{-1}, STP)
A	41	48 (@423K)
A	48	51 (@423K)
A	49	47 (@423K)
A	50	54 (@423K)
B	17	28 (@423K)
B	21	28 (@423K)
B	23	40 (@423K)
B	25	35 (@423K)
B	26	26 (@423K)
B	27	133 (@323K)
B	124	122 (@323K)
B	184	135 (@323K)
C	0	250 (@323K)
C	7	193 (@323K)
C	8	170 (@323K)
C	11	154 (@323K)

Table S2. Independent N_2 adsorption measurements for the Mo_2C samples listed in Table 1. These data were used to calculate the data listed in Table 1.

Catalyst	aging time (days)	BET surface area ($m^2\ g^{-1}$)	micropore surface area ($m^2\ g^{-1}$)†	micropore volume ($\times 10^{-3}$ $cm^3\ g^{-1}$)§
A	110	23.1	15.6	8.0
A	116	26.1	18.0	8.9
A	118	23.9	17.8	8.9
B	63	18.4	8.27	4.2
B	64	17.9	9.27	4.6

† estimated from t-plot method
§ estimated at the relative pressure $P/P° = 0.98$

5 nm

(a)   (b)
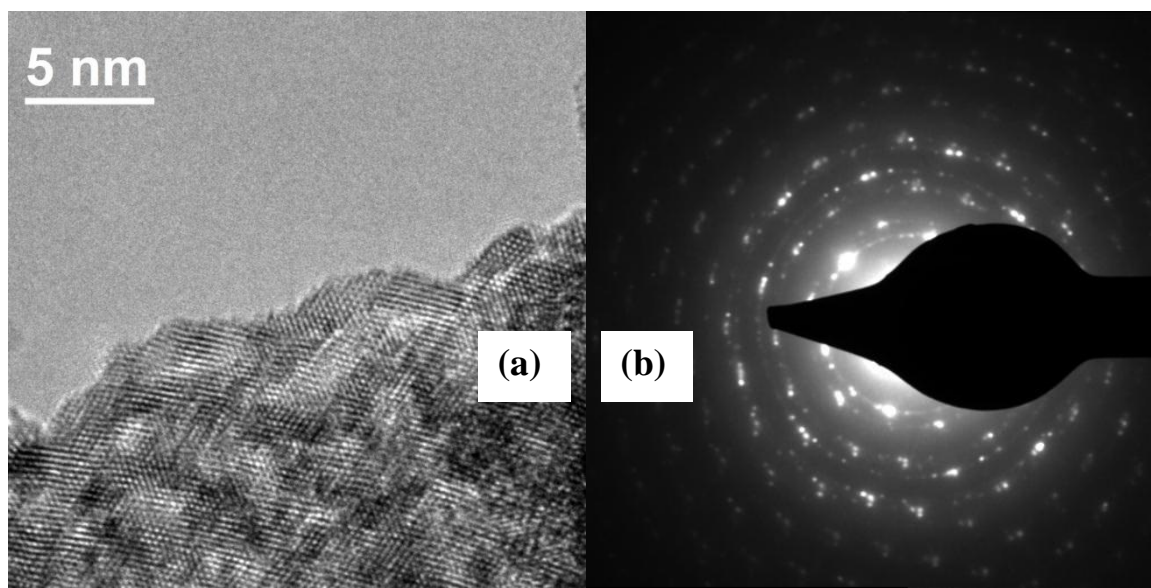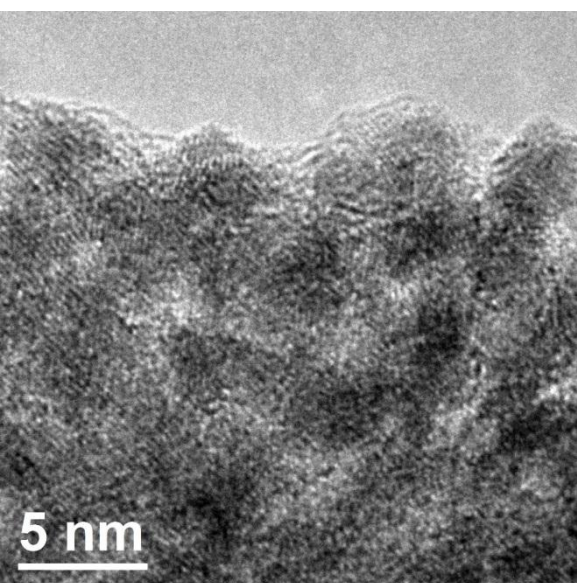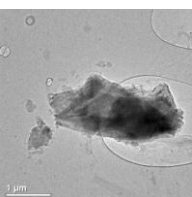
(c)

Figure S1. TEM images for (a) representative fresh, passivated Mo_2C catalyst (sample A in Table 1) and (b) the corresponding selected area electron diffraction (SAED) of a chosen fresh, passivated Mo_2C particle (shown in the inset), and a TEM image for (c) spent Mo_2C catalyst after kinetic measurements shown in Figure 4 (sample A in Table 1).
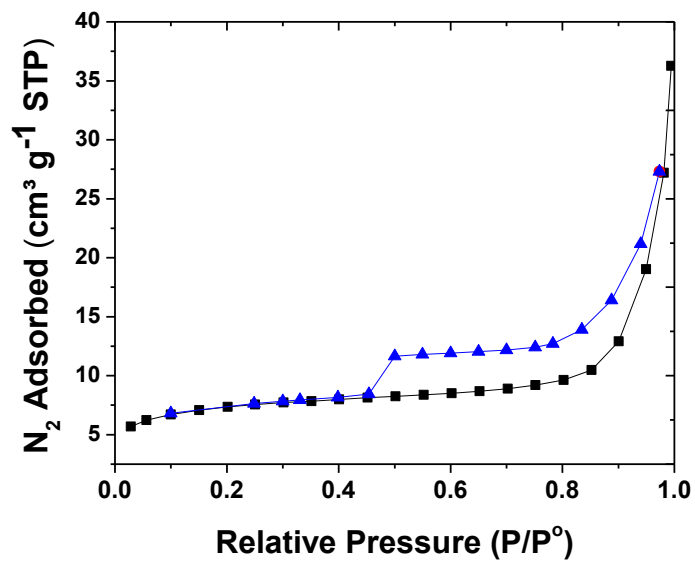
Figure S2. N_2 adsorption (square)/desorption (triangle) isotherm at 77 K for a representative Mo_2C catalyst (sample A in Table 1).

2. Kinetic measurements of vapor phase furfural hydrodeoxygenation on Mo_2C catalysts

2.1. Absence of external mass transfer and heat transfer limitations

The absence of external mass transfer and heat transfer limitations was checked by estimating Mears' criteria. Since the catalyst deactivated with time on stream, furfural conversion ~15% was chosen as the upper bound of the observed reaction rate (furfural consumption rate). External mass transfer limitations can be neglected if the Mears' criterion listed below is satisfied [1]:

$$\frac{-r_{A(obs)} \times \rho_b \times R \times n}{k_c \times C_{Ab}} < 0.15$$

where $-r_{A(obs)}$ is the observed reaction rate in kmol kg_{cat}^{-1} s^{-1}; ρ_b is catalyst bed density = $(1-\Phi)\,\rho_c$ in kg m^{-3} (ρ_c = density of catalyst pellet in kg m^{-3}, which is reported to be ~760 kg $m^{-3[2]}$, Φ = porosity of the catalyst bed); R is the catalyst pellet radius in m; n is the reaction order of reactant A; C_{Ab} is the concentration of reactant A in the bulk gas phase at 420 K in kmol m^{-3}; k_c is the mass transfer coefficient for reactant A. Since the Reynolds number for this system, defined as Re = $2U \times R \times \rho/\mu$ (where U is superficial velocity in m s^{-1}, ρ is the density of the reactant mixture fluid, estimated using H_2 at 420 K, μ is the viscosity of the reactant mixture fluid, estimated using H_2 at 420 K), is much smaller than 1, the mass transfer coefficient (k_c) was estimated by assuming Sh (Sherwood number) = $k_c \times (2R)/D_e$ = 2 (where De = estimated diffusivity of reactant A in the bulk gas phase [3]). Table S3 lists the parameters used for the Mears' criterion calculation as well as the estimated values for the external mass transfer limitation using either furfural or H_2 as reactant A. The absence of external mass transfer limitations was confirmed by the Mears' criterion calculation.

Heat transfer limitations can be neglected if the Mears' criterion listed below is satisfied [1]:

$$\frac{-r_{A(obs)} \times \rho_b \times R \times E \times (-\Delta H_{rxn})}{R_g \times h \times T^2} < 0.15$$

where $-r_{A(obs)}$ is the observed reaction rate in kmol kg_{cat}^{-1} s^{-1}; ρ_b is the catalyst bed density = (1-Φ) ρ_c in kg m^{-3} (ρ_c = density of catalyst pellet in kg m^{-3}, which is reported to be ~760 kg m^{-3}[2], Φ = porosity of the catalyst bed); R is the catalyst pellet radius in m; E is the activation energy of the reaction in kJ $kmole^{-1}$; $-\Delta H_{rxn}$ is the heat of the reaction in kJ $mole^{-1}$; R_g is the universal gas constant = 8.314 x 10^{-3} kJ $mole^{-1}$ K^{-1}; h is the heat transfer coefficient in W $(m^2-K)^{-1}$; T is the reaction temperature = 423 K. Since the Reynolds number for this system is much smaller than 1, the heat transfer coefficient was estimated by assuming Nu (Nusselt number) = h⨯ (2R)/kt = 2 (where kt = thermal conductivity of the reactant mixture fluid, estimated using H_2 at 423 K). Table S3 shows the parameters used for the Mears' criterion calculation as well as the estimated values to evaluate heat transfer limitations for the furfural HDO reaction. The absence of heat transfer limitations was confirmed by the Mears' criterion calculation.

Table S3. Parameters used in the Mears' criterion for estimating external mass transfer limitations in vapor phase furfural hydrodeoxygenation (HDO) reaction for furfural (in parentheses) or hydrogen as the primary reactant.

Parameters	External mass transfer	Heat transfer
Reaction rate at 423 K: $-r_{A(obs)}$ (kmol kg_{cat}^{-1} s^{-1})[a]	~2.5 x10^{-7}	~2.5 x10^{-7}
density of catalyst pellet: ρ_c (kg m^{-3})	~760	~760
catalyst bed density: $\rho_b=(1-\Phi)x\rho_c$ (kg m^{-3})	~532 (Φ= porosity, estimated~0.3)	~532 (Φ= porosity, estimated~0.3)
radius of catalyst pellet: R (m)	~1.5x10^{-4}	~1.5x10^{-4}
bulk gas concentration of H_2 (or furfural) at 420 K: kmol m^{-3}	~2.9 x10^{-2} (~7 x10^{-5})	~2.9 x10^{-2} (~7 x10^{-5})
Reynolds number: Re[b]	~3.3 x 10^{-2}	~3.3 x 10^{-2}
estimated diffusivity of D_{AB} for the H_2–furfural system [3]:(m^2 s^{-1})	6.3 x 10^{-5}	
mass transfer coefficient for furfural or H_2: kc (m s^{-1})[c]	0.4	
reaction order of furfural (H_2): n	~0.3 (~0.5)	
heat of reaction: $\Delta Hrxn$ (kJ $mole^{-1}$)[d]		-167
activation energy (kJ $kmole^{-1}$)		83000
estimated thermal conductivity (pure H_2 at 423 K): kt (W $(m\text{-}K)^{-1}$)		1.9 x 10^{-1}
heat transfer coefficient: h (W $(m^2\text{-}K)^{-1}$)[e]		1.3 x 10^{3}
Estimated Mears' criterion[f]	2 x 10^{-4} (1 x10^{-6})	2 x10^{-7}

a: assuming furfural conversion ~15% with catalyst loading ~0.1 g
b: superficial velocity = 0.021 m s^{-1} (flow rate ~1.67 cm^3 s^{-1} through a reactor with inner diameter~ 0.01 m), estimated fluid kinematic viscosity (~pure H_2 at 423 K): ~ 1.9 x 10^{-4} (m^2 s^{-1})
c: Since Re << 1, mass transfer coefficient was estimated by assuming Sh (Sherwood number)=kc(2R)/D_{AB}=2, where R=catalyst pellet radius and D_{AB} =gas phase diffusivity for the H_2–furfural system
d: estimated from primary reaction : $C_5H_4O_2 + 2H_2 \rightarrow C_5H_6O + H_2O$
e: Since Re << 1, heat transfer coefficient was estimated by assuming Nu (Nusselt number)=h(2R)/kt=2, where R=catalyst pellet radius and kt = thermoconductivity of the reactant mixture fluid
f: for heat transfer limitations, reaction temp= 423 K, universal gas constant = 8.314 x 10^{-3} (kJ $mole^{-1}$ K^{-1})

2.2. Absence of internal mass transfer limitations

The internal mass transfer limitation was checked by estimating the Thiele modulus. The Thiele modulus (ϕ) was calculated from the following equation:

$$\Phi = \frac{-r_{A(obs)} \times \rho_c \times R^2}{D_e \times C_{As}} = \eta\phi^2$$

where $-r_{A(obs)}$ is the observed reaction rate in kmol kg_{cat}^{-1} s^{-1}; ρ_c is the pellet bulk density of Mo_2C catalyst, which is reported to be ~760 kg m^{-32}, R is the catalyst pellet radius in m; D_e is the effective diffusivity at 420 K in m^2 s^{-1}. C_{As} is the gas concentration of reactant A at the catalyst surface in kmol m^{-3}, η is the internal effectiveness factor and ϕ is the Thiele modulus. If $\phi \ll 1$, then $\eta \approx 1$ and ϕ can be calculated. An iterative calculation shows that ϕ values do not exceed 0.1. The parameters used for the Thiele modulus calculation are listed in Table S4

Table S4. Parameters used in the estimation of the Thiele modulus in vapor phase furfural hydrodeoxygenation (HDO) reaction for furfural (in parentheses) or hydrogen as the primary reactant.

Parameters	Catalyst pellet
Reaction rate (kmole s^{-1} k$_{Cat}$$^{-1}$)[a]	~2.5x10^{-7}
Density of catalyst pellet:ρ_c (kg m^{-3})	~760
Radius of catalyst pellet:R (m) [b]	1.5x10^{-4}
Effective diffusivity : De (m^2 s^{-1})[c]	3.3x10^{-6}
Estimated Thiele modulus for anisole HDO reaction[d]	(0.08) 0.003

a: assuming furfural conversion ~15% with catalyst loading ~0.1 g
b: estimated from the average of mesh size between 40 (400 µm) and 80 (177 µm)
c: The diffusivity of D$_{AB}$ for the furfural-H$_2$ system was estimated to be ~6.3 x10^{-5} m^2 s^{-1} [3]. We note that *Knudsen diffusivity* was not used here because the average diameter of the pores in the catalyst pellet was found to be >20 nm (from BJH desorption branch), which is much larger than that of the reactant molecules. The constriction factor of 0.8, pellet porosity of 0.35 and tortuosity of 6 were considered in the estimation of the effective diffusivity.
d: gas concentration of furfural and H$_2$ at the catalyst surface at ~423 K: ~6.9 x10^{-5} and ~2.9 x10^{-2} kmol m^{-3} respectively.

2.3. Correction for catalyst deactivation to obtain apparent reaction H_2

Since Mo_2C catalyst deactivates during vapor phase furfural HDO reactions (as shown in Figure 4), a correction for catalyst deactivation needs to be carried out to obtain kinetic parameters such as apparent H_2 order and apparent activation energy that reflect intrinsic catalytic behaviour. Two different methods were used to assess the consequence of catalyst deactivation on measured reaction rates. The first method involved the choice of a standard condition and its use as a reference at a given time-on-stream. After measurement of 2MF STY at process reaction conditions other than the standard condition (i.e., at a different reaction temperatures or reactant partial pressures), the reaction conditions were restored to the chosen standard condition and the corresponding 2MF STY was measured. The extent of catalyst deactivation was assessed by calculating the ratio of the 2MF STY at standard conditions measured at those two different time-on-stream. The corrected 2MF STY measured at varying temperature and partial pressure conditions were then obtained by multiplying the extent of catalyst deactivation. An example for calculating apparent H_2 order is illustrated below with detailed data shown in Table S5. The data obtained at 24.8 ks with H_2 partial pressure ~0.98 atm (2MF STY ~2.30 $x10^{-8}$ mole s^{-1} g_{cat}^{-1}) was chosen as a reference. After measuring the 2MF STY at H_2 partial pressure ~0.66 (25.9 ks time-on-stream), the reaction conditions were set back to standard conditions (H_2 partial pressure ~0.98 atm) and the corresponding 2MF STY is 2.18 $x10^{-8}$ mole s^{-1} g_{cat}^{-1} (27.0 ks time-on-stream). The extent of catalyst deactivation is, therefore, 2.30/2.18 ~ 1.06. The 2MF STY was then measured at H_2 partial pressure ~0.14 atm (28.1 ks time-on-stream) with raw data ~0.64 $x10^{-8}$ mole s^{-1} g_{cat}^{-1}. The corrected 2MF STY measured at H_2 partial pressure ~0.14 atm was calculated as (0.64 $x10^{-8}$) x 1.06 = ~0.68 $x10^{-8}$ mole s^{-1} g_{cat}^{-1}. A similar methodology was then applied to the following experiments (experiment set #2 to #7 shown in Table S5) and the corrected 2MF STY measured at different H_2 partial pressures from experiment sets #2-7 together with the data obtain from experiment #1 was used to obtain the apparent H_2 order, which is ~0.56 (data points , ∘ , shown in Fig. S6). Figure S4 also provides the corresponding visualization of 2MF production rate at different conditions (raw data (◯), measured at

the standard condition ($\blacklozenge$) and corrected 2MF rate ($\star$) based on experimentally measured 2MF rate at the standard condition) vs. time-on-stream.

The second method is illustrated as follows: one can fit the raw data measured at a chosen standard condition to obtain a deactivation curve. Figure S5 shows a deactivation curve constructed based on data before 25 ks ($\blacksquare$) (shown in Table S5). This deactivation curve was then used to predict the corresponding 2MF STY at the time when the 2MF STY was measured at conditions other than the standard condition. For example, while 2MF STY measured at 28.1 ks time-on-stream was at H_2 partial pressure 0.14 atm, one can assess the predicted 2MF STY under the standard condition at 28.1 ks time-on-stream using the aforementioned deactivation curve, which was 1.82 $\times 10^{-8}$ mole s^{-1} g_{cat}^{-1}. By using the same reference point (2MF STY ~2.30 $\times 10^{-8}$ mole s^{-1} g_{cat}^{-1} at 24.8 ks time on stream), the extent of catalyst deactivation can be evaluated and was found to be: 2.3/1.82 = ~1.26. The corrected 2MF STY measured at H_2 partial pressure ~0.14 atm was calculated as (0.64 $\times 10^{-8}$) x 1.26 = ~0.81 $\times 10^{-8}$ mole s^{-1} g_{cat}^{-1}. The corrected 2MF STY measured at different H_2 partial pressures from experiment sets #2-#7 was then obtained using the same methodology. The apparent H_2 order obtained using this method was found to be 0.51 (data points , $\triangle$, shown in Fig. S7), which is very close to the value obtained via the first method (~0.56). Figure S6 also provides corresponding visualization of 2MF production rate at different conditions (raw data ($\blacksquare$), predicted 2MF rate at standard condition using the deactivation curve shown in Fig. S5 ($\times$), and the corrected 2MF production rate ($\star$)) versus time-on-stream. Since no significant differences between these two methods for assessment of the effects of deactivation on measured kinetics were noted, all kinetics measured in this work were corrected for catalyst deactivation by re-measuring the 2MF STY at the standard condition every time.

Figure S3. 2MF production rate per gram of catalyst as a function of time. Fresh Mo_2C catalyst (□) and the same catalyst after the first (◁) and second (○) regeneration cycle. Reaction conditions: furfural/CH_4/H_2 vol% = ~0.24%/2.5%/bal (total flow rate ~1.67 cm^3 s^{-1}), reaction temperature ~423 K under ambient pressure. The kinetic data of Mo_2C catalysts for vapor phase furfural HDO was first reported in our previous work,[4] it has been re-plotted in this work.

Table S5. 2MF production rate data, experimental conditions and catalyst deactivation correction for apparent H_2 order measurement

Exp. Set [†]	Time (ks)	H_2 partial pressure (atm)	conditions	raw data for 2MF production rate (x10^{-8} mole s^{-1} g$_{cat}$$^{-1}$)	corrected 2MF production rate based on experimentally measured 2MF production rate at standard condition (x10^{-8} mole s^{-1} g$_{cat}$$^{-1}$)[†]	Predicted 2MF production rate under standard condition (STD) at when the catalysts was tested under different reaction conditions based on the deactivation curve (x10^{-8} mole s^{-1} g$_{cat}$$^{-1}$)	corrected 2MF production rate based on the predicted 2MF production rate at the standard condition (x10^{-8} mole s^{-1} g$_{cat}$$^{-1}$)[‡]
	5.4	0.98	STD	23.00			
	7.6	0.98	STD	12.88			
	9.7	0.98	STD	7.72			
	11.9	0.98	STD	5.64			
	13.0	0.98	STD	5.06			
	15.1	0.98	STD	4.49			
	17.3	0.98	STD	3.93			
	20.5	0.98	STD	3.07			
	22.7	0.98	STD	2.49			
1	24.8	0.98	STD	2.30	2.30		2.30
1	25.9	0.66		1.77	1.77		1.77
2	**27.0**	**0.98**	**STD**	**2.18**			
2	28.1	0.14		0.64	0.68	1.82	0.81
3	**29.2**	**0.98**	**STD**	**1.94**			
3	30.2	0.11		0.62	0.74	1.63	0.88
4	**31.3**	**0.98**	**STD**	**1.95**			
4	32.4	0.08		0.46	0.55	1.47	0.72
5	**33.5**	**0.98**	**STD**	**1.90**			
5	34.6	0.45		1.14	1.39	1.34	1.97
	35.6	0.98	STD	1.81			
6	**36.7**	**0.98**	**STD**	**1.76**			
6	37.8	0.77		1.46	1.91	1.18	2.87
7	**38.9**	**0.98**	**STD**	**1.66**			
7	40.0	0.21		0.64	0.89	1.08	1.36

† catalyst deactivation was monitored by retesting the catalyst at a chosen standard condition (STD). The 2MF production rate measured at different H_2 partial pressure was adjusted for the deactivation by reference to the original STD condition (exp. set #1) using experimentally measured 2MF production rate at the standard condition. For example, the corrected 2MF rate for exp. Set#2 would be 0.64*2.30/2.18 = 0.68. The corrected 2MF production rate was used to calculate the apparent hydrogen order.

‡ The 2MF production rate measured at different H_2 partial pressures was adjusted for deactivation by reference to the original STD condition (exp. set #1) based on a predicted 2MF production rate under the standard condition at when the catalyst was measured at conditions other than standard conditions using the deactivation curve determined with the data points before 25 ks time on stream. Therefore, the corrected 2MF rate for exp. Set#2 would be 0.64*2.30/1.82 = 0.81. The corrected 2MF production rate was used to calculate the apparent hydrogen order.

Figure S4. 2MF production rate (raw data (○), 2MF rate measured at the standard condition (♦) and corrected 2MF rate (★) based on experimentally measured 2MF rate at the standard condition) vs. time-on-stream. H_2 pressure varied from ~0.1 to ~1 atm (balance He) at ~0.24 kPa furfural at 423 K. Reaction conditions: furfural/CH_4/H_2 vol% = ~0.24%/2.5%/bal (total flow rate ~1.67 cm^3 s^{-1}), space velocity ~2.6 cm^3 s^{-1} g$_{cat}$$^{-1}$ and catalyst loading ~0.64 g (sample A in Table 1).
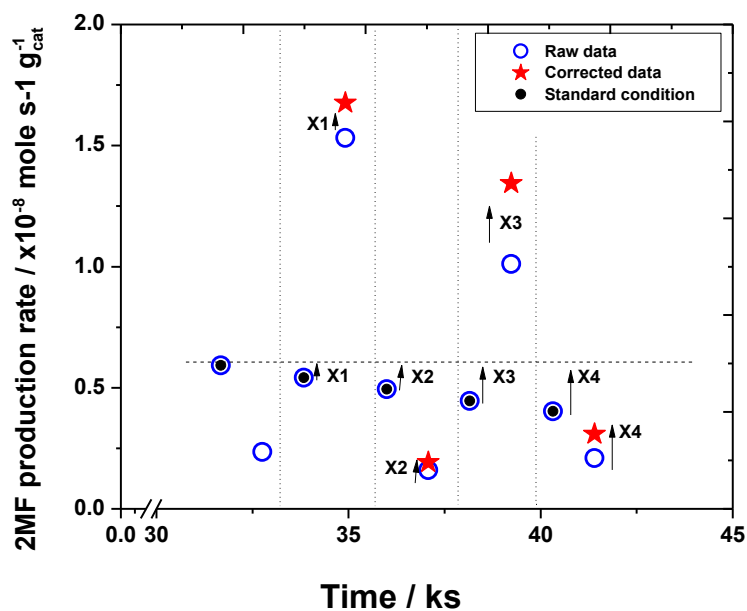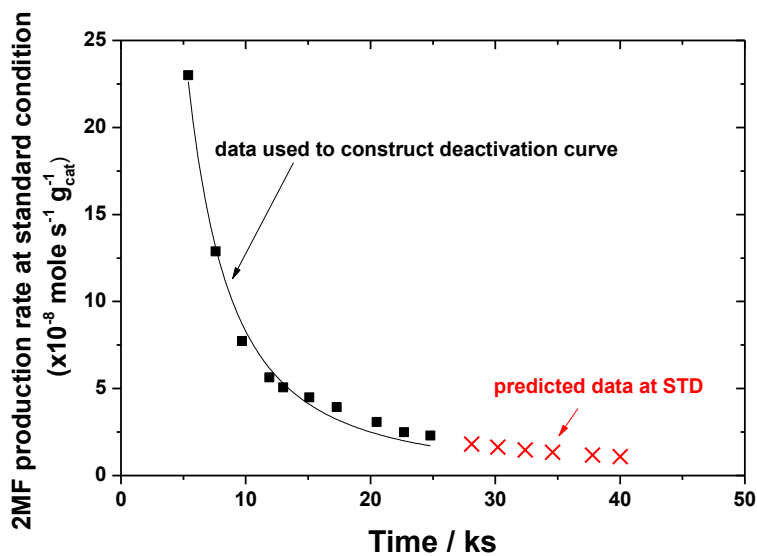
Figure S5. 2MF production rate vs. time-on-stream for a typical Mo_2C catalyst. The data before 25 ks (■, which corresponds to the data shown in Table S5) were used to construct a deactivation curve, which was used to predict the 2MF STY (×) at the given time when the catalysts were tested under different temperature and pressure conditions (which corresponds to the experiment sets #1 to #7 shown in Table S5).
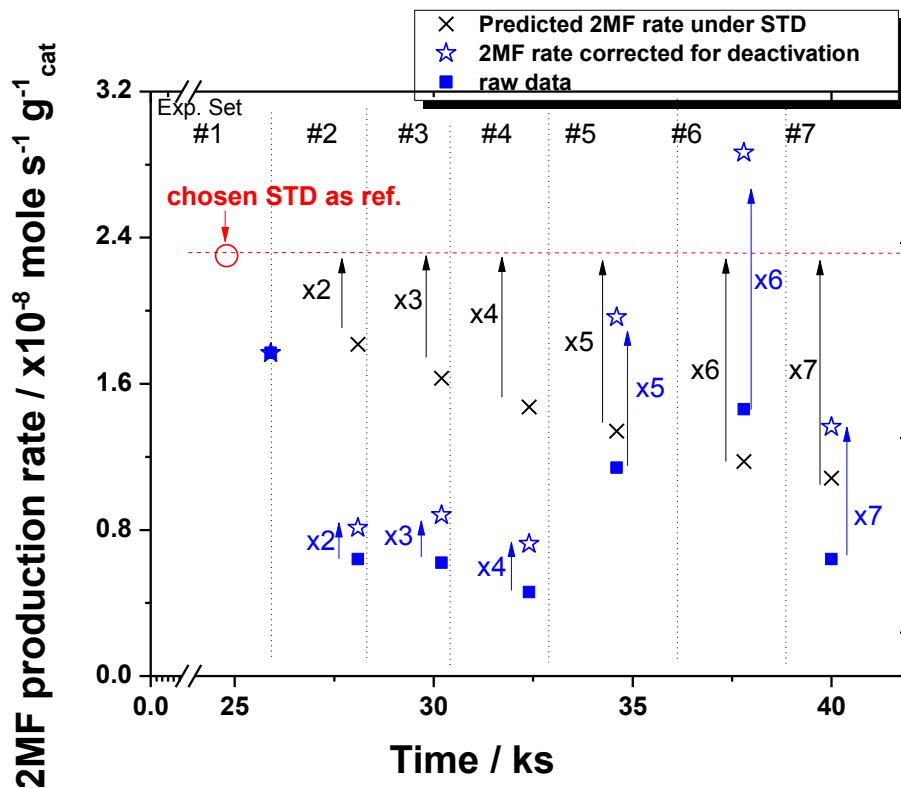
Figure S6. 2MF production rate (raw data (■), predicted 2MF rate at standard condition using the deactivation curve shown in Fig. S5 (✕) and corrected 2MF rate (☆) vs. time-on-stream. H_2 pressure varied from ~0.1 to ~1 atm (balance He) at ~0.24 kPa furfural at 423 K. Reaction conditions: furfural/CH_4/H_2 vol% = ~0.24%/2.5%/bal (total flow rate ~1.67 cm^3 s^{-1}), space velocity ~2.6 cm^3 s^{-1} g_{cat}^{-1} and catalyst loading ~0.64 g (sample A in Table 1).
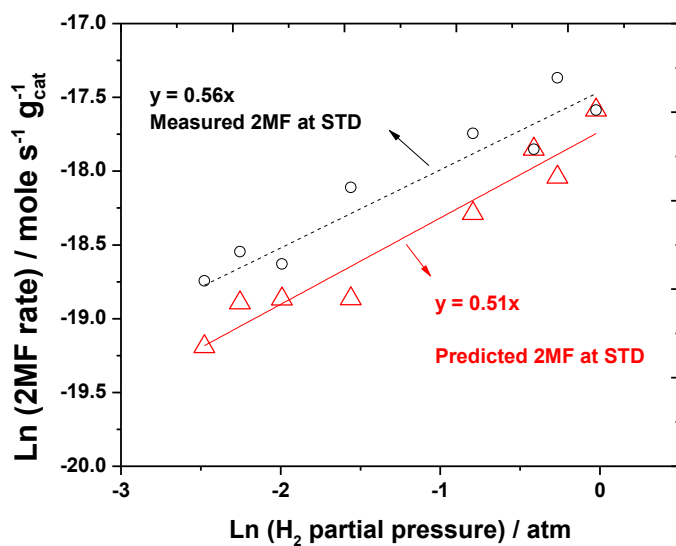
Figure S7. H$_2$ order plot (varied from ~0.1 to ~1 atm (balance He) at ~0.24 kPa furfural at 423 K) obtained by using experimentally measured 2MF production rate at the standard condition (○) and predicted 2MF production rate at the standard condition (△) for catalyst deactivation correction. (H$_2$ varied from ~0.1 to ~1 atm (balance He) at ~0.24 kPa furfural at 423 K) Reaction conditions: furfural/CH$_4$/H$_2$ vol% = ~0.24%/2.5%/bal (total flow rate ~1.67 cm^3 s^{-1}), space velocity ~2.6 cm^3 s^{-1} g$_{cat}^{-1}$ and catalyst loading ~0.64 g (sample A in Table 1). See Table S5 for detailed data.
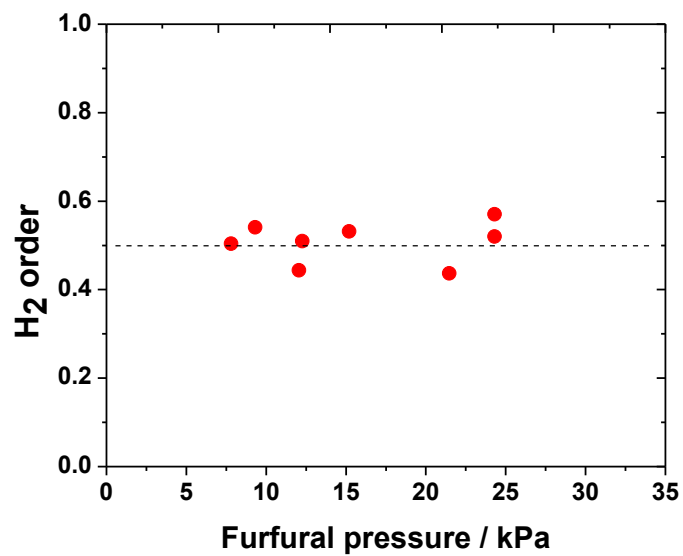
Figure S8. H_2 order of 2MF production rates at different furfural concentrations (5-25 kPa).   Experimental data obtained at 423 K, H_2 pressure varied from ~0.1 to ~1 atm (balance He) with CH_4 as internal standard, total pressure =1 atm.

2.4. Correction for catalyst deactivation to obtain apparent activation energy

Apparent activation energy can also be obtained after correcting the catalyst deactivation by the aforementioned method used for the apparent H_2 order. An example for calculating apparent activation energy is illustrated below with a detailed data set shown in Table S6. The data obtained at 31.7 ks with reaction temperature ~423 K (2MF STY ~0.59 $\times 10^{-8}$ mole s^{-1} g_{cat}^{-1}) was chosen as a reference. After measuring the 2MF STY at reaction temperature ~409 K (32.8 ks time on stream), the reaction conditions were set back to standard conditions (reaction temperature ~423 K) and the corresponding 2MF STY is 0.54 $\times 10^{-8}$ mole s^{-1} g_{cat}^{-1} (33.8 ks time on stream). The extent of catalyst deactivation is, therefore, 0.59/0.54 ~ 1.09. The 2MF STY was then measured at reaction temperature ~443 K (34.9 ks time on stream) with raw data ~1.53 $\times 10^{-8}$ mole s^{-1} g_{cat}^{-1}. The corrected 2MF STY measured at reaction temperature ~443 K was calculated as (1.53 $\times 10^{-8}$) x 1.09 ~ 1.67$\times 10^{-8}$ mole s^{-1} g_{cat}^{-1}. A similar methodology was then employed for the following experiments (experiment sets #2 to #5 shown in Table S5) to get the corrected 2MF STY measured at different reaction temperatures. The apparent activation energy for a typical Mo_2C catalyst (sample A in Table 1) was found to be ~86 kJ mole^{-1} and the corresponding Arrhenius plot is shown in Figure S9.

Table S6. 2MF production rate data, experimental conditions, and catalyst deactivation correction for apparent activation energy measurement

Exp. Set †	Time (ks)	Temperature (K)	conditions	raw data for 2MF production rate $(x10^{-8}$ mole s^{-1} g$_{cat}^{-1})$	corrected 2MF production rate $(x10^{-8}$ mole s^{-1} g$_{cat}^{-1})$†
1	31.7	423	STD	0.59	0.59
1	32.8	409		0.23	0.23
2	**33.8**	**423**	**STD**	**0.54**	
2	34.9	443		1.53	1.67
3	**36**	**423**	**STD**	**0.49**	
3	37.1	404		0.16	0.19
4	**38.2**	**423**	**STD**	**0.45**	
4	39.2	438		1.01	1.34
5	**40.3**	**423**	**STD**	**0.40**	
5	41.4	412		0.21	0.31

†The 2MF production rate measured at different reaction temperatures was adjusted for deactivation by reference to the original standard condition (exp. set #1) using experimentally measured 2MF production rates at the standard condition. The corrected 2MF production rate was used to assess the apparent activation energy reported.
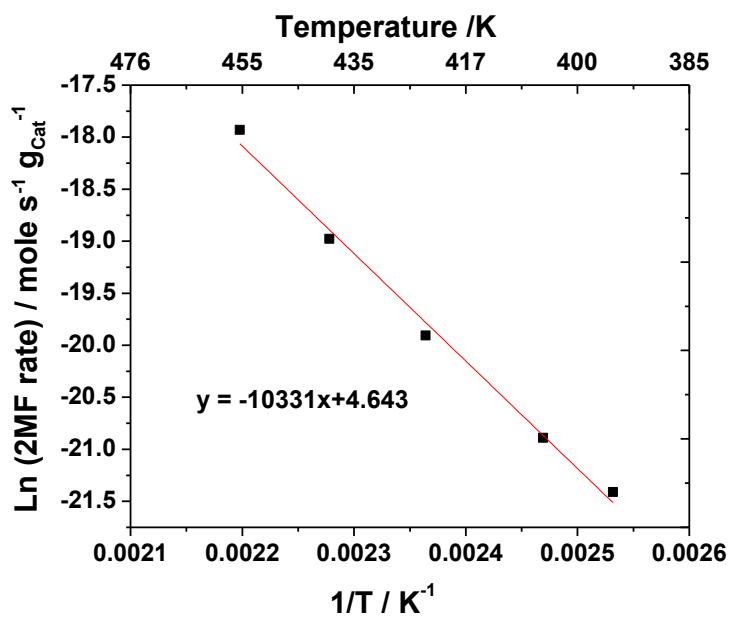
Figure S9.   Effect of temperature (feed composition: furfural/CH_4/H_2 vol% = ~0.24%/2.5%/bal) on 2MF production rate for a typical Mo_2C catalyst (sample A in Table 1).   The kinetic data were corrected for catalyst deactivation by reference to a chosen standard condition (See Table S6 for detailed data). Experimental data obtained at total pressure =1 atm

3. Derivation of 2MF production rate equation

3.1. Mechanism 1 (step 1-9)

Considering step 3 (Eq. (3)) is RDS, the rate equation for 2MF production can be expressed as

$$r_{2MF} = k_3 \frac{z}{L_1}[H - S_1][R - CHO - S_2]$$

where k_3 represents the forward rate constant, $z[H–S_1]/L_1$ represents the probability of finding adjacent $[R\text{-}CHO\text{-}S_2]$ surface species to $[H\text{-}S_1]$ species, L_1 represents the total number of active sites S_1, and $[R\text{-}CHO\text{-}S_2]$ and $[H\text{-}S_1]$ denote surface concentrations of dissociated hydrogen on site S_1 and furfural adsorbed on S_2, respectively. Since all the other steps are assumed to be in quasi-equilibrium, so

$$[H - S_1] = K_1^{1/2}[S_1][H_2]^{1/2}$$

$$[R - CHO - S_2] = K_2 \ [S_2][R - CHO]$$

Considering site balance for S_1 and S_2,

$$[L_1] = [S_1] + [H - S_1]$$

$$\begin{aligned}[L_2] = {}&[S_2] + [R - CHO - S_2] + [R - CHOH - S_2] + [R - CH - S_2] \\ &+ [OH - S_2] + [R - CH_2 - S_2] + [R - CH_3 - S_2] + [H_2O \\ &- S_2]\end{aligned}$$

and the most abundant reactive intermediate (MARI) for site 1 (S_1) is empty sites and the coverage of the adsorbed furfural intermediate, R-CHO-S_2, is much higher than that for the rest of the species adsorbed on S_2 sites

$$[L_1]\sim[S_1] \gg [H-S_1]$$

$$[L_2] \sim [R-CHO-S_2]$$
$$\gg ([S_2]+[R-CHO-S_2]+[R-CHOH-S_2]$$
$$+[R-CH-S_2]+[OH-S_2]+[R-CH_2-S_2]$$
$$+[R-CH_3-S_2]+[H_2O-S_2])$$

$$\text{Therefore, } [L_2]\sim[R-CHO-S_2] = K_2\ [S_2][R-CHO]$$

$$[S_2] \sim \frac{[L_2]}{K_2\ [R-CHO]}$$

Substitute the expression of [R-CHO-S_2], [H-S_1], [S_1] and [S_2] derived above, the rate equation for 2MF production with half order in H_2 and zero order in furfural, therefore, can be obtained

$$r_{2MF} = k_3\ \frac{z}{L_1}K_1^{1/2}[S_1][H_2]^{1/2}K_2\ [S_2][R-CHO]$$

$$r_{2MF} = k_3\ \frac{z}{L_1}K_1^{1/2}[L_1][H_2]^{1/2}K_2\ \frac{[L_2]}{K_2\ [R-CHO]}[R-CHO]$$

$$r_{2MF} = k_3\ z\ K_1^{1/2}[L_2][H_2]^{1/2}[R-CHO]^0$$

3.2. Mechanism 2 (step 1,2,10-14,8-9)

Alternatively, if we consider step 10 (Eq. (10)) is RDS, the rate equation for 2MF production can be expressed as

$$r_{2MF} = k_{11} \frac{z}{L_1} [H - S_1][R - CH - S_2]$$

where k_{11} represents the forward rate constant, $z[H–S_1]/L_1$ represents the probability of finding adjacent [R-CH-S_2] surface species to [H-S_1] species, L_1 represents the total number of active sites S_1, and [R-CH-S_2] and [H-S_1] denote surface concentrations of dissociated hydrogen on site S_1 and furfural adsorbed on S_2, respectively. Since all the other steps are assumed to be in quasi-equilibrium, so

$$[H - S_1] = K_1^{1/2}[S_1][H_2]^{1/2}$$

$$[R - CH - S_2][O - S_2] = K_{10}[S_2][R - CHO - S_2]$$

$$[R - CHO - S_2] = K_2 \, [S_2][R - CHO]$$

and from step 8 and 9 amd 14, one can get

$$[H_2O][S_1][S_2] = K_8 \, K_9 \, [OH - S_2][H - S_1]$$

$$[H_2O][S_1][S_2] = K_8 \, K_9 \, [OH - S_2]K_1^{1/2}[S_1][H_2]^{1/2}$$

$$[H_2O][S_2] = K_8 \, K_9 \, [OH - S_2]K_1^{1/2}[H_2]^{1/2}$$

$$[HO - S_2][S_1] = K_{14}[H - S_1][O - S_2]$$

Therefore, the expression for $[O - S_2]$ can be solved:

$$[O - S_2] = K_1^{-1}K_8^{-1}K_9^{-1}K_{14}^{-1}[H_2]^{-1}[H_2O][S_2]$$

And

$$[R - CH - S_2]$$

$$= K_1^1 K_8^1 K_9^1 K_{14}^1 K_2 K_{10}[H_2][H_2O]^{-1}[S_2][R - CHO]$$

Considering site balance for S_1 and S_2,

$$[L_1] = [S_1] + [H - S_1]$$

$$[L_2] = [S_2] + [R - CHO - S_2] + [R - CH - S_2] + [O - S_2] + [OH - S_2]$$
$$+ [R - CH_2 - S_2] + [R - CH_3 - S_2] + [H_2O - S_2]$$

and the most abundant reactive intermediate (MARI) for site 1 (S_1) is empty sites and the coverage of the adsorbed furfural intermediate, R-CHO-S_2, is much higher than that for the rest of the species adsorbed on S_2 sites

$$[L_1] \sim [S_1] \gg [H - S_1]$$

$$[L_2] \sim [R - CH - S_2]$$
$$\gg ([S_2] + [R - CHO - S_2] + [O - S_2] + +[OH - S_2]$$
$$+ [R - CH_2 - S_2] + [R - CH_3 - S_2] + [H_2O - S_2])$$

Therefore,

$$[L_2] \sim [R - CH - S_2] = K_1^1 K_8^1 K_9^1 K_{14}^1 K_2 K_{10}[H_2][H_2O]^{-1}[S_2][R - CHO]$$

$$[S_2] \sim \frac{[L_2]}{K_1^1 K_8^1 K_9^1 K_{14}^1 K_2 K_{10}[H_2][H_2O]^{-1}[R-CHO]}$$

Substitute the expression of [R-CH-S_2], [H-S_1], [S_1] and [S_2] derived above, the rate equation for 2MF production with half order in H_2 and zero order in furfural, therefore, can be obtained

$$r_{2MF} = k_{11}\frac{Z}{L_1}[H-S_1][R-CH-S_2]$$

$$= k_{11}\frac{Z}{L_1}K_1^{1/2}[S_1][H_2]^{1/2} \quad K_1^1 K_8^1 K_9^1 K_{14}^1 K_2 K_{10}[H_2][H_2O]^{-1}[S_2][R$$
$$- CHO]$$

$$= k_{11}z\,K_1^{1/2}[H_2]^{1/2}\ [R-CHO]^0\ [L_2]$$

4. References:

1.   H. S. Fogler, *Elements of Chemical Reaction Engineering*, Prentice - Hall PTR Upper Saddle River, NJ, 2006.
2.   E. A. Blekkan, P. H. Cuong, M. J. Ledoux and J. Guille, *Industrial & Engineering Chemistry Research*, 1994, **33**, 1657-1664.
3.   R. B. Bird, W. E. Stewart and E. N. Lightfoot, *Transport Phenomena*, John Wiley & Sons, Inc, 605 Third Avenue, New York, 2002.
4.   K. Xiong, W.-S. Lee, A. Bhan and J. G. Chen, DOI: 10.1002/cssc.201402033,*ChemSusChem*.in press